J. Fluid Mech. (2002), *vol.* 456, *pp.* 219–237.
DOI: 10.1017/S0022112001007479 Printed in the United Kingdom

The nonlinear properties of a large-scale dynamo driven by helical forcing

By FAUSTO CATTANEO[1], DAVID W. HUGHES[2] AND JEAN-CLAUDE THELEN[3]

[1]Department of Mathematics, University of Chicago, Chicago, IL 60637, USA

[2]Department of Applied Mathematics, University of Leeds, Leeds LS2 9JT, UK

[3]Department of Astronomy and Astrophysics, University of Chicago, Chicago, IL 60637, USA

(Received 16 November 2000 and in revised form 22 August 2001)

By considering an idealized model of helically forced flow in an extended domain that allows scale separation, we have investigated the interaction between dynamo action on different spatial scales. The evolution of the magnetic field is studied numerically, from an initial state of weak magnetization, through the kinematic and into the dynamic regime. We show how the choice of initial conditions is a crucial factor in determining the structure of the magnetic field at subsequent times. For a simulation with initial conditions chosen to favour the growth of the small-scale field, the evolution of the large-scale magnetic field can be described in terms of the α-effect of mean field magnetohydrodynamics. We have investigated this feature further by a series of related numerical simulations in smaller domains. Of particular significance is that the results are consistent with the existence of a nonlinearly driven α-effect that becomes saturated at very small amplitudes of the mean magnetic field.

1. Introduction

Magnetic fields are responsible for a host of astrophysical phenomena, over a vast range of spatial scales (Parker 1979). In the Sun, for example, the solar cycle provides evidence of a global, coherent field on the one hand, whereas, on the other, magnetic fields are observed all the way down to the limits of spatial resolution. The evolution of cosmical magnetic fields is most naturally explained in terms of dynamo action, in which the fields are amplified and maintained by the motions of an electrically conducting fluid. The study of dynamo action has addressed this problem from many different points of view. Consideration of the physical processes involved has led to the distinction, *inter alia*, between kinematic and dynamic, slow and fast, and large- and small-scale dynamos. Furthermore, this has led to the development of approximations that afford conceptual or computational advantages for certain specific cases.

A kinematic dynamo is one in which the magnetic field is weak, in the sense that the velocity field is independent of the Lorentz force. Kinematic dynamos describe the initial amplification of magnetic fields from a state of weak magnetization. By contrast, in a dynamic dynamo the magnetic field, through the Lorentz force, plays a dynamical role. Dynamic dynamos describe the saturation and subsequent maintenance of magnetic fields over long periods of time. Kinematic dynamos are traditionally studied within the framework of the *kinematic approximation*, in which the evolution of the (weak) magnetic field is described by solution of the induction equation alone, for prescribed velocities. This clearly affords an enormous simplification in

that the problem of solving the Navier–Stokes equation is side-stepped altogether, and the dynamo aspects are reduced to what is, in essence, a linear eigenvalue problem for the dynamo growth rate. Interestingly, and as we shall see later, there are circumstances in which the kinematic regime is not adequately described by the kinematic approximation.

The distinction between slow and fast dynamos is peculiar in that it only rigorously applies to kinematic dynamos; specifically, a dynamo is said to be fast if its growth rate remains positive in the limit of infinite electrical conductivity, and is said to be slow otherwise. From a physical point of view, it is perhaps more sensible to distinguish not so much between fast and slow, but between dynamos that operate in fluids with high as opposed to low electrical conductivity (measured in dimensionless units by the magnetic Reynolds number Rm). The latter distinction applies both to the kinematic and dynamic regimes, and corresponds to actual situations of physical interest; for example, in most laboratory experiments the magnetic Reynolds numbers is low, whereas in the majority of astrophysical situations it is huge.

The distinction between large- and small-scale dynamos relates to the spatial structure of the generated magnetic fields. A large-scale dynamo generates magnetic fields with characteristic scales large compared with those of the velocity. A small-scale dynamo, by contrast, generates magnetic fields with characteristic scales smaller than, or comparable to, those of the velocity. Most cosmical magnetic fields have a well-defined large-scale component, typically being generated by a combination of large-scale and small-scale motions. Toroidal magnetic field is generated by the large-scale shearing, due to differential rotation, of the poloidal magnetic field; the large-scale poloidal field is regenerated through the cumulative effects of small-scale motions acting on the toroidal field. *Mean field electrodynamics* was developed specifically to study the evolution of magnetic fields driven, at least in part, by small-scale motions. A certain mathematical elegance of this approach, together with its 'user friendliness', has led to practically all studies of astrophysical dynamos being cast within its framework. One of the assumptions of mean field theory, possibly one that is not always explicitly stated (though see the discussions in Moffatt 1978 and Krause & Rädler 1980), is that the small-scale fields are stable to dynamo growth. Indeed, for low magnetic Reynolds number turbulence lacking reflectional symmetry (e.g. helical turbulence), it is indeed the case that there will be dynamo amplification of the large-, but not the small-scale field. However, at high or even moderate magnetic Reynolds numbers the situation is likely to be more complex. Recent advances in dynamo theory, mostly driven by the fast dynamo issue, suggest that small-scale dynamo action is very prevalent even in the absence of helicity (see, for example, Hughes, Cattaneo & Kim 1996). Thus, turbulence in highly (electrically) conducting fluids is always likely to act as a small-scale dynamo, and in the presence of helicity, as a large-scale dynamo also.

The aim of the work described in this paper is to investigate the important issue of the interplay between magnetic field generation on different spatial scales. We base our approach on moderately high magnetic Reynolds number simulations of helically forced flows, in which we follow in detail the magnetic field evolution in both the kinematic and dynamic regimes. Rather than attack the problem in its full generality, an approach that is simply not feasible even with present resources, we consider a somewhat idealized model that nevertheless captures the essence of scale separation. The following section contains the formulation of the model problem. In § 3 we study the evolution of the magnetic field from initial states of weak magnetization, through the kinematic and into the dynamic regime, addressing, in particular, the importance

of initial conditions. We find that in one case the results can be understood in terms of the classical α-effect of mean field electrodynamics, a point that is investigated by a further series of calculations in § 4. A critical discussion of the results is contained in § 5.

2. Formulation

We consider dynamo action in an incompressible fluid with constant electrical conductivity and viscosity. The evolution equations in dimensionless form and standard notation can be written as

$$(\partial_t - Re^{-1}\nabla^2)\boldsymbol{U} + \boldsymbol{U}\cdot\nabla\boldsymbol{U} = -\nabla p + \boldsymbol{J}\times\boldsymbol{B} + \boldsymbol{F}, \tag{2.1}$$

$$(\partial_t - Rm^{-1}\nabla^2)\boldsymbol{B} = \nabla\times(\boldsymbol{U}\times\boldsymbol{B}), \tag{2.2}$$

$$\nabla\cdot\boldsymbol{B} = \nabla\cdot\boldsymbol{U} = 0, \tag{2.3}$$

where $\boldsymbol{F}$ is a forcing function, and Re and Rm are the kinetic and magnetic Reynolds numbers respectively. The choice of $\boldsymbol{F}$ determines, to a large extent, the character of the problem. Since we are interested here in the transition from kinematic to nonlinear dynamo states we choose a particular forcing function that leads to a kinematic regime with properties that are well understood. To this end, we define $\boldsymbol{F}$ in terms of $\boldsymbol{U}_0$, where

$$\boldsymbol{U}_0 = (\partial_y\psi, -\partial_x\psi, \psi), \quad \psi = \sqrt{3/2}[\cos(x+\cos t) + \sin(y+\sin t)], \tag{2.4}$$

and

$$\boldsymbol{F} = (\partial_t - Re^{-1}\nabla^2)\boldsymbol{U}_0. \tag{2.5}$$

This construction guarantees that in the absence of magnetic field, $\boldsymbol{U} = \boldsymbol{U}_0$ is a solution of the momentum equation (2.1). This can easily be verified by noting that $\nabla\cdot\boldsymbol{U}_0 = 0$, and that $\boldsymbol{U}_0$ is maximally helical ($\boldsymbol{U}_0\times(\nabla\times\boldsymbol{U}_0) = 0$) so that $\boldsymbol{U}_0\cdot\nabla\boldsymbol{U}_0$ is the gradient of a scalar.

The velocity $\boldsymbol{U}_0$ was introduced by Galloway & Proctor (1992) in the context of kinematic dynamo theory, and has a number of interesting properties. The flow $\boldsymbol{U}_0$ is triply-periodic and z-independent; as a result, the induction equation has separable solutions of the form

$$\boldsymbol{B}(\boldsymbol{x}, t) = \boldsymbol{B}_p(x, y, t)\exp(st + \mathrm{i}k_z z), \quad s = \sigma + \mathrm{i}\omega, \tag{2.6}$$

where $\boldsymbol{B}_p$ is periodic in time with the same period as $\boldsymbol{U}_0$. This form of the solution affords a formal reduction of the induction equation from three to two spatial dimensions. In fact, it was this very property that led several authors to choose this general type of velocity as the basis for their studies of kinematic dynamo action (e.g. Galloway & Proctor 1992; Otani 1993; Cattaneo *et al.* 1995; Ponty, Pouquet & Sulem 1995; Hughes *et al.* 1996). In the simplest case where $\boldsymbol{B}_p$ has the same spatial periodicity as $\boldsymbol{U}_0$, the maximum growth rate (taken over all values of k_z) increases with Rm before levelling off at a value of approximately 0.3 at $Rm \approx 80$. Significantly, increases in Rm up to the level of computational feasibility ($Rm \approx 10^5$) leave the growth rate unaffected. This led Galloway & Proctor (1992) to conjecture that it would indeed remain unaffected in the limit $Rm \to \infty$ – the fast dynamo property. In general, the growth rate depends both on the wavenumber k_z and on Rm. Remarkably, however, provided that Rm is sufficiently large ($\gtrsim 50$), the mode of maximum growth rate becomes independent of Rm, assuming the value $k_z \approx 0.57$; in other words the mode of maximum growth rate attains asymptotically a fixed 'size'.

This should be contrasted with, for instance, the time-independent version of (2.4), for which, as $Rm \to \infty$, the maximum growth rate tends to zero (albeit slowly, as $\ln(\ln Rm)/\ln Rm$) (Soward 1987). Furthermore, in this latter case, the wavenumber of maximum growth rate increases with Rm, the scale of the mode of fastest growth decreasing to zero (as $((\ln Rm)/Rm)^{1/2}$) as Rm becomes infinite. The difference between these two cases is attributed to the presence of large regions of chaotic streamlines in the time-dependent flow, and their absence in the steady case.

In the present paper our interests are chiefly in the nonlinear regime, where we anticipate that the problem will become three-dimensional and that therefore we will lose the computational advantage afforded by two-dimensionality. The motivation for our choice of forcing function is thus somewhat different. We wish to study the development of nonlinear dynamo states from initial conditions of weak magnetization and so as a first consideration it makes sense to build upon a well-studied kinematic regime. We note that this is not merely a matter of choosing a convenient velocity, but rather of choosing one that is hydrodynamically robust. In other words, it should be possible to drive the chosen velocity for times that are long compared to the typical growth time of the magnetic field. The time-dependent flow (2.4) falls into this category, in contrast, interestingly, to *steady ABC* flows for which instability can set in at quite low values of the fluid Reynolds number (for the $A = B = C = 1$ flow, instability sets in at $Re \approx 13$ (Podvigina & Pouquet 1994)). As a second factor, the forcing function $\boldsymbol{F}$ given by (2.5) gives rise to a spatially periodic problem that can be efficiently implemented numerically. Third, even at moderate Rm the velocity $\boldsymbol{U}_0$ is a healthy dynamo (for $k_z = 0.57$, dynamo action sets in at $Rm \approx 1.5$), and thus the nonlinear regime can be attained in a reasonably short computational time. Fourth, and crucially for the work described in the following section, the dynamo growth rate remains positive as $k_z \to 0$. This implies that the velocity $\boldsymbol{U}_0$ can amplify magnetic fields with arbitrarily large extent in the z-direction. Finally, we conclude this section by noting that since, by computational necessity, nonlinear studies are restricted to moderate values of Rm, we do not explicitly invoke the fast dynamo property of $\boldsymbol{U}_0$. Nonetheless, it gives us hope that the results derived here may apply even in the large-Rm regime.

2.1. *Numerical considerations*

The equations (2.1)–(2.3) with the forcing function defined by (2.4)–(2.5) can be efficiently solved on a triply-periodic domain by standard pseudo-spectral techniques. Spatial derivatives are evaluated in phase space where they reduce to simple wavevector multiplications. Nonlinear terms involving products of the field variables are evaluated in configuration space where, once again, they reduce to simple multiplications. Aliasing errors are removed by standard 2/3 rule methods. The diffusive terms can be treated exactly by use of an integrating factor. For the overall time discretization we adopt a third-order Runge–Kutta scheme. The pressure term in (2.1) is not explicitly evaluated; instead, the updated velocity is constrained to be solenoidal by an exact phase-space projection method. The transformation between phase and configuration space is afforded by fast Fourier transform techniques optimized for parallel architectures.

3. Tall boxes

In this section we explore the interplay between the evolution of magnetic structures of different sizes. In particular, we are interested in the conditions that lead to the

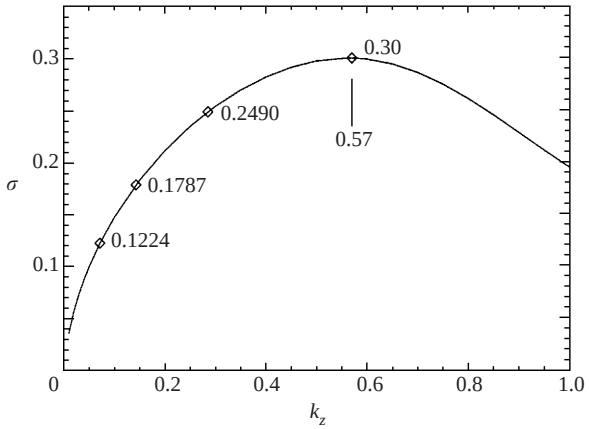

FIGURE 1. Dynamo growth rate as a function of vertical wavenumber k_z for a case with $Rm = 100$. The value of the maximum growth rate and of selected overtones ($k_z = 0.57/2$, $k_z = 0.57/4$ and $k_z = 0.57/8$) are shown.

generation of large-scale magnetic fields. As a natural starting point for our discussion we consider the dependence of the growth rate on the 'vertical' wavenumber k_z. (For convenience we shall refer to z as the vertical, and x and y as the horizontal directions, even though there is no gravity in this problem.) This dependence, for $Rm = 100$, is shown in figure 1. The growth rate has a maximum at $k_z = k_{max} \approx 0.57$, decreasing monotonically to zero at $k_z = 0$. Significantly, $\mathrm{d}\sigma/\mathrm{d}k_z(k_z = 0) > 0$, so that there is exponential growth for magnetic fields of arbitrarily large vertical extent. For $k_z > k_{max}$ the curve decreases to zero non-monotonically, its detailed structure depending on Rm (Hughes, Cattaneo & Kim 1998). By contrast, the behaviour for small k_z is found to be surprisingly insensitive to changes in Rm. The properties of the associated eigenfunctions have been extensively studied (Cattaneo *et al.* 1995) and will not be reviewed here except to note that the horizontal components of $\boldsymbol{B}_p$ in expression (2.6) have non-zero horizontal averages. In other words, the horizontally averaged structure of the kinematic eigenfunctions is that of a horizontal uniform field, the direction of which varies with z. We shall refer to this property presently.

Since we are mostly concerned with the interaction between large- and small-scale magnetic structures it is appropriate to specify precisely what we mean by these terms in the present context. Typically in dynamo theory, scales are defined relative to the characteristic scale of the velocity. In the case of turbulent flows this scale naturally corresponds to the correlation length. For the flow $\boldsymbol{U}_0$, the only meaningful scale is that of the horizontal periodicity since the flow is z-independent. However, it would be misleading to equate this particular scale with a correlation length, since for periodic flows all periodic subdomains are in phase and hence, in some sense, the correlation length is infinite. Instead, for this problem it is more meaningful to shift the emphasis from the velocity to the magnetic field. The horizontal structure of the magnetic eigenfunction is not appropriate since, as mentioned above, the horizontal average is non-zero, and therefore the magnetic field can be thought of as having infinite extent. On the other hand, the vertical extent of the mode of maximum growth rate is a well-defined, meaningful scale, and we shall adopt it here as the scale characterizing this problem. As we shall see shortly, there are dynamical reasons why this is a particularly appropriate choice. Thus, a large-scale field is to be understood as one with *vertical* extent large compared to that of the mode of maximum growth rate.

I.C.	U_{rms}	B_{rms}
$A_1 \gg A_8$	1.35	0.85
$A_1 \approx A_8$	1.34	0.82

TABLE 1. The root-mean-square velocity U_{rms} and root-mean-square magnetic field B_{rms} for the tall box runs, with $Re = Rm = 100$, dimensions $2\pi \times 2\pi \times 16\pi/k_{max}$ and resolution $128 \times 128 \times 1024$.

We are now in a position to describe our numerical experiments. Details of the runs are given in table 1. We consider a computational domain of size 2π in the x- and y-directions, and $8 \times 2\pi/k_{max}$ in the z-direction. Such a domain houses, for example, eight replicas of the mode of maximum growth rate or the mode with vertical wavenumber $k_{max}/8$ exactly once. This choice is motivated by a compromise between the need for a scale separation worthy of the name and computational feasibility. It is convenient, in this section, to define a new vertical wavenumber K measured in units of $k_{max}/8$; with this notation the mode of maximum growth rate has $K = 8$. As initial conditions we impose

$$\boldsymbol{U}(\boldsymbol{x}, 0) = \boldsymbol{U}_0(\boldsymbol{x}, 0), \quad \boldsymbol{B}(\boldsymbol{x}, 0) = A_1 \boldsymbol{B}_p^{(1)} \mathrm{e}^{\mathrm{i}z} + A_8 \boldsymbol{B}_p^{(8)} \mathrm{e}^{8\mathrm{i}z}, \tag{3.1}$$

where $\boldsymbol{B}_p^{(K)}$ describes the horizontal structure of the kinematic eigenmode of wavenumber K (cf. (2.6)). If the constants A_1, $A_8 \ll 1$ then, initially, the Lorentz force will be negligible and the velocity will satisfy $\boldsymbol{U}(\boldsymbol{x}, t) \approx \boldsymbol{U}_0(\boldsymbol{x}, t)$. Initially, the magnetic field will evolve kinematically, before eventually attaining sufficient strength that the Lorentz force becomes dynamically significant. The subsequent evolution is essentially nonlinear and of particular interest to the present study. Clearly, the structure of the magnetic field as it enters this nonlinear phase depends on the initial choice of the amplitudes A_1 and A_8. We explore this dependence by considering two distinct cases, one in which the large-scale field becomes dynamical while the small-scale field is still kinematic, and another in which the roles are reversed.

3.1. *Large-scale saturation*

We consider first a case in which the initial amplitudes A_1 and A_8 are chosen such that the energy in the large-scale component exceeds the energy in the small-scale component throughout the kinematic regime. The transition to the dynamical regime and the subsequent development can be followed by the time evolution of the (magnetic) energy density binned by vertical wavenumber. Thus we define

$$M_K(t) = \frac{1}{2} \sum_{k_x, k_y} |\hat{\boldsymbol{B}}(k_x, k_y, K)|^2, \tag{3.2}$$

where $\hat{\boldsymbol{B}}$ is the Fourier transform of $\boldsymbol{B}$; no distinction is made here between positive and negative values of K. Similar quantities V_K can be defined analogously for the velocity. Figure 2(a) shows the time evolution of the total magnetic energy, and that of some specific wavenumbers; figure 2(b) shows the corresponding curves for the total kinetic energy, V_0 and V_2. Two important epochs can be identified: $t = t_d \approx 12$, corresponding to the beginning of the dynamical regime and characterized by substantial departures from an exponential behaviour; $t = t_s \approx 35$, corresponding to the beginning of the stationary state. The interval $t_d < t < t_s$ is a period of dynamical readjustment in which the system evolves markedly from the kinematic state. The ratio M_1/M_8 is approximately 100 at $t = t_d$ implying that, at least initially,

the modification to the velocity is due entirely to the Lorentz force associated with the large-scale field component. Interestingly, this ratio decreases only slightly during the period $t_d < t < t_s$; thus, even after the nonlinear readjustment, the energy in the large-scale component substantially exceeds that of the small-scale component.

It is useful to note that in the kinematic regime, although the Lorentz force is dynamically negligible, it has important symmetry-breaking consequences. During the kinematic phase of the evolution the energy growth in wavenumbers other than 1 and 8 is dominated by nonlinear interactions. For instance, the initial production of magnetic energy in wavenumber 3 (see figure 2*a*) can be understood as follows. The Lorentz force associated with the $K = 1$ eigenfunction drives a weak velocity with wavenumber $K = 2$; the interaction between this velocity component and the $K = 1$ eigenfunction leads to the excitation of the $K = 3$ mode. Similarly, the initial energy growth of wavenumbers 6 and 12 is associated with a weak velocity with wavenumber 9, itself driven by the Lorentz force due to the cross-interaction between the eigenfunctions with wavenumbers $K = 1$ and 8, and the magnetic field mode with $K = 3$ described above. From the preceding examples it is easy to deduce that initial conditions with even or odd parity are preserved for all times. Thus, both even and odd wavenumbers must be present initially to obtain a complete spectrum. In the kinematic regime there are two distinct contributions to the growth of each mode. One is the intrinsic dynamo instability of the system and proceeds at the dynamo growth rate for that particular mode. The other is due to nonlinear interactions and can, in many circumstances, exceed the natural dynamo growth rate. For example, in the present case, the growth of the $K = 1$ and 8 modes in what we define to be the kinematic regime is mostly due to the former, while for all other modes it is due to the latter.

The evolution can be summarized as follows. There is a kinematic phase in which the $K = 1$ and 8 modes are growing exponentially at the dynamo growth rate, and all other modes are being amplified nonlinearly. The initial conditions are such that the $K = 1$ mode is the first to reach sufficient amplitude to be dynamically significant, leading to a modification of the velocity field such that its own exponential growth is saturated. There then follows an intermediate phase in which all other modes increase to their equilibrium amplitude. The resulting state is one in which the large-scale field, $K = 1$ here, is dominant; all other modes are present at a substantially lower amplitude. From this example one would conclude that the dynamo system under consideration can efficiently generate a large-scale magnetic field.

3.2. *Small-scale saturation*

We now consider the opposite case in which the initial amplitudes A_1 and A_8 are chosen such that the energy in the small-scale component exceeds that in the large-scale component throughout the kinematic regime. Figure 3 shows the evolution of the energies binned by wavenumber. By analogy with the previous example, we introduce $t_d \approx 20$ and $t_s \approx 65$ signifying, respectively, the times at which the magnetic field becomes dynamically significant and at which the system enters a statistically stationary state. The evolution of the $K = 8$ mode proceeds in a similar way to that of the $K = 1$ mode in the previous case; the energy grows exponentially in the kinematic regime, overshoots and then declines in the readjustment phase between t_d and t_s, eventually settling down to its stationary value. Likewise, the $K = 1$ mode grows exponentially in the kinematic phase, is further amplified in the readjustment phase, and finally saturates at a level that is substantially less than that of the $K = 8$ mode. Superficially, it would appear that the present case is analogous to the previous

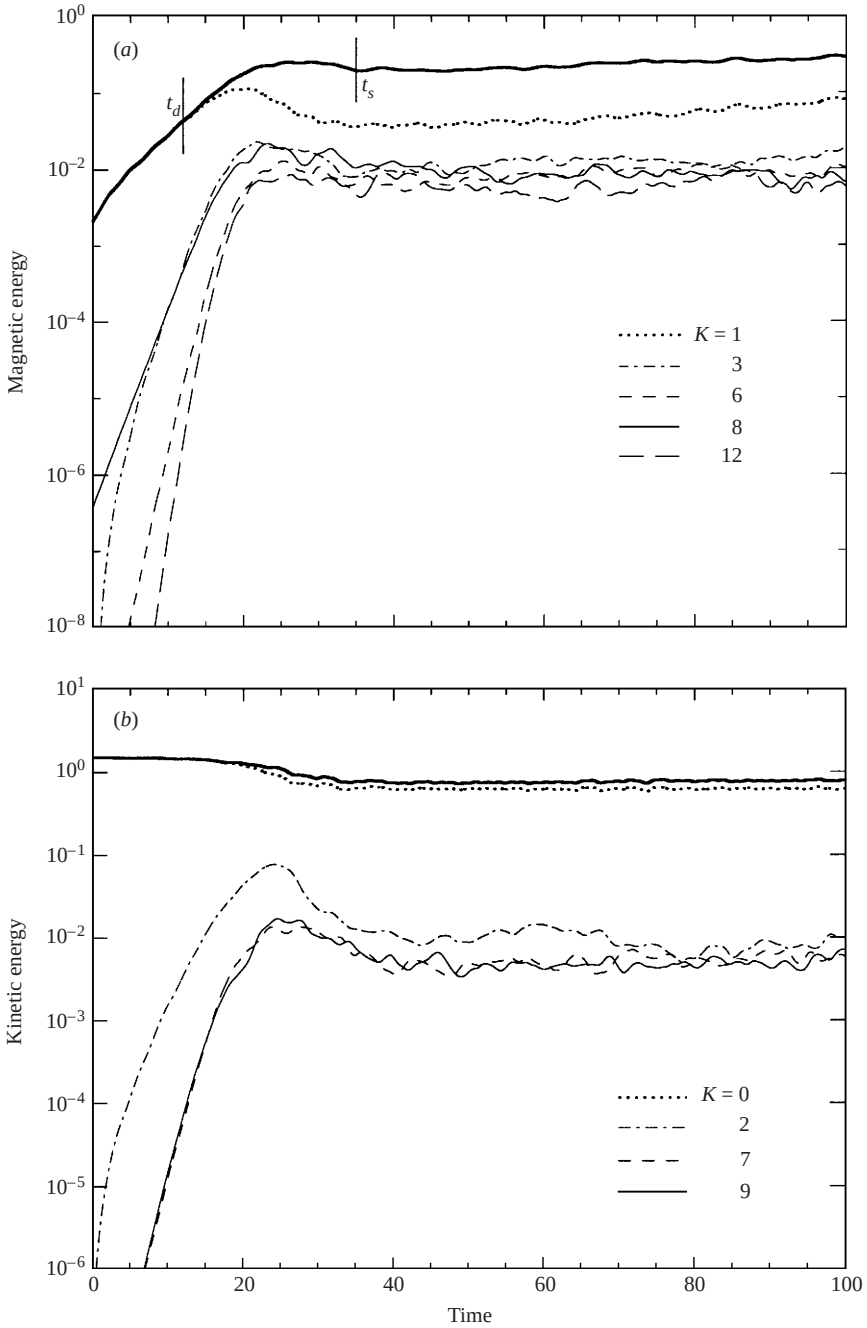

FIGURE 2. Time evolution of (*a*) the magnetic and (*b*) kinetic energies as functions of time for a case with $Rm = 100$. The magnetic initial conditions were such that $A_1(0) \gg A_8(0)$. Also shown are the time histories of the energies binned by vertical wavenumbers for specific choices of wavenumbers. Notice that, after the nonlinear saturation, the magnetic energy in the $K = 1$ bin considerably exceeds that in any other bin.

one, only with the roles of the $K = 1$ and $K = 8$ modes reversed. However, we should note that there is a fundamental difference between them; whereas the nonlinear amplification of modes with $K > 1$ in the previous case corresponds to a *forward* cascade, the amplification of modes with $K < 8$ in the present case corresponds to a *backward* cascade. This is exemplified by consideration of the evolution of the $K = 1$ mode (see inset in figure 3*a*). For times less than $t = t_1 \approx 20$ the mode grows exponentially at its natural dynamo growth rate. At $t = t_1$ the contributions to the mode energy due to nonlinear interactions exceed that of the dynamo instability and the energy begins to grow at a higher rate. This accelerated growth continues up to $t = t_2 \approx 40$, after which the mode gradually approaches its stationary value. During the period $t_1 < t < t_2$ the dominant nonlinear contributions to the energy growth of the $K = 1$ mode are due to the interaction between magnetic fluctuations with $K = 8$ and velocity fluctuations with $K = 7$ and 9, the latter being driven by the Lorentz force associated with the interaction between the $K = 1$ and $K = 8$ modes. (We believe that the equality between t_d and t_1 is coincidental.) The significant feature to note is that the nonlinear contributions to the *large-scale* field ($K = 1$ mode) can be represented as spatial averages of products of *small-scale* fluctuations ($K = 7, 8, 9$). These have the form of the familiar α-effect term of mean field electrodynamics, and it is therefore tempting to interpret them within the framework of this theory.

To examine this issue more closely, it is helpful to consider the different physical mechanisms that can lead to the growth of the $K = 1$ mode; thus, symbolically, we may write

$$(\partial_t - Rm^{-1}\nabla^2)\boldsymbol{b}_1 = \nabla \times (\boldsymbol{u}_0 \times \boldsymbol{b}_1 + \alpha \boldsymbol{b}_1 + \boldsymbol{Q}_1). \tag{3.3}$$

Here $\boldsymbol{b}_1$ represents the amplitude of the $K = 1$ mode, $\boldsymbol{u}_0$ is the z-independent part of the velocity, which at least initially is close to $\boldsymbol{U}_0$, α measures the strength of the α-effect arising from the interaction between fluctuating quantities, and $\boldsymbol{Q}_1$ is a remainder. For small $|\boldsymbol{b}_1|$ we expect $\boldsymbol{u}_0$ and α to be independent of $\boldsymbol{b}_1$, but possibly depending on the fluctuations, while we expect $\boldsymbol{Q}_1$ to be of order $|\boldsymbol{b}_1|^2$. We emphasize that equation (3.3) should be understood only as a convenient way of expressing the relative importance of the production terms. During the kinematic phase the α term grows approximately exponentially due to the growth of fluctuations, overtaking the kinematic growth (the $\boldsymbol{u}_0$ term) at $t = t_1$. For $t_1 < t < t_2$ the growth of the large-scale field is dominated by the α-effect, the efficiency of which decreases dramatically after $t = t_2$. This picture, and the saturation amplitude of the large-scale field, are consistent with the idea of strong suppression of the α-effect (Vainshtein & Cattaneo 1992; Kulsrud & Anderson 1992; Gruzinov & Diamond 1995; Cattaneo & Hughes 1996), a point that will be pursued further in the next section. From this example, and in sharp contrast to the previous case, one would conclude that the dynamo system under consideration cannot efficiently generate a large-scale magnetic field.

The nature of the α-effect just invoked is somewhat non-standard and merits further examination. The α-effect is based on the assumption that a scale separation exists between mean and fluctuating fields, and expresses a relationship between the mean electromotive force and the mean field. Traditionally, this relationship is most clearly described within the framework of kinematic theory in which the velocity fluctuations are prescribed (i.e. they are independent of magnetic effects), and small-scale magnetic fluctuations arise from the interaction between the mean field and the fluctuating velocity. The linearity of the equation for the magnetic fluctuations with respect to both the mean and fluctuating fields then implies a relationship of the form

$$\mathscr{E} = \langle \delta \boldsymbol{u} \times \delta \boldsymbol{b} \rangle = \alpha \boldsymbol{B} + \ldots, \tag{3.4}$$

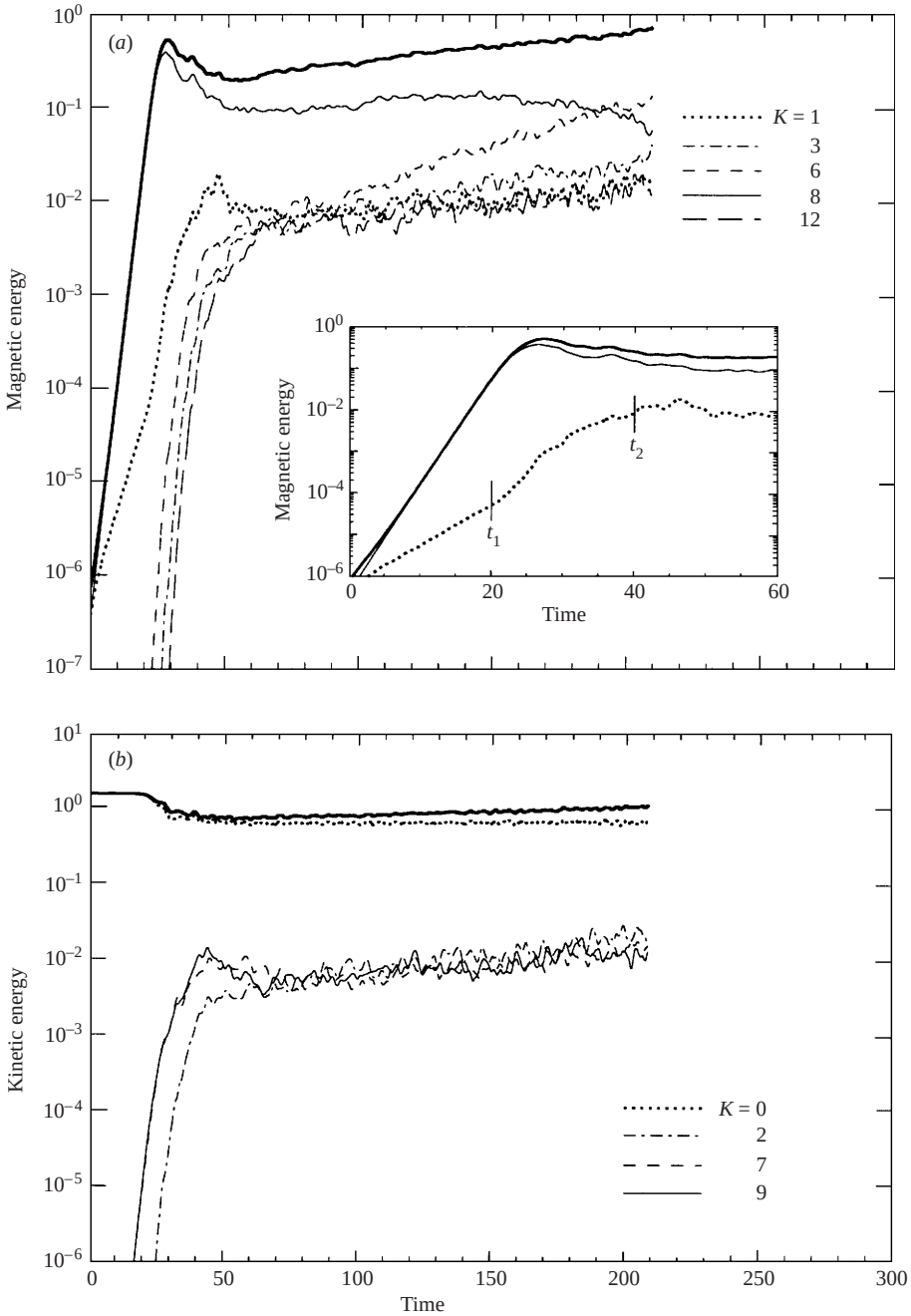

FIGURE 3. Time evolution of (*a*) the magnetic and (*b*) kinetic energies as functions of time for a case with $Rm = 100$. The magnetic initial conditions were such that $A_1(0) \approx A_8(0)$. Also shown are the time histories of the energies binned by vertical wavenumbers for specific choices of wavenumbers. The inset in (*a*) shows the evolution for early times of the magnetic energy in the wavenumber $K = 1$ and 8 bins, and of the total (magnetic) energy.

where $\boldsymbol{B}$ is the mean field, $\delta\boldsymbol{u}$ and $\delta\boldsymbol{b}$ are the fluctuating velocity and magnetic field respectively, and the dots represent terms involving (spatial) derivatives of the mean field. An underlying, but not often stated assumption (though, see Moffatt 1978 and Krause & Rädler 1980), is that the magnetic fluctuations arise solely through the interaction between the mean field and the fluctuating velocity. This should be contrasted with the present case in which the magnetic fluctuations are unstable in their own right, and therefore their amplitude is largely independent of the mean field amplitude, at least when the latter is weak. Furthermore, here, the velocity fluctuations are not prescribed, but rather are driven by the interaction between the mean and fluctuating fields. Thus expression (3.4) still holds in an approximate sense, although the roles of $\delta\boldsymbol{u}$ and $\delta\boldsymbol{b}$ are reversed, i.e. the magnetic fluctuations are prescribed (independent of the mean field) while the velocity fluctuations are driven by the mean field. In general, because of the intrinsic nonlinearity of the Navier–Stokes equations, we do not expect a linear relationship between $\delta\boldsymbol{u}$ and $\boldsymbol{B}$ except, possibly, at small Reynolds numbers. Thus we are led to the counterintuitive result that the α-effect depends on the mean field even in the kinematic regime.

4. Short boxes

One of the more remarkable features to emerge in the previous section is that one aspect of the evolution of the large-scale field in the second experiment described above can be conveniently interpreted in terms of an α-effect. Since the notion of the α-effect has been of central importance to our understanding of the generation of cosmic magnetic fields, and given further that there appears to be some controversy regarding its efficiency in the dynamical regime, we should take advantage of the situation and pursue the matter further. The aim of this section is to establish convincingly that a measurable effect is present, corresponding to our intuitive idea of the α-effect, and to measure its dependence on the defining parameters, namely the strength of the mean field and the magnetic Reynolds number.

It would be tempting to use the results of the previous section to measure the average electromotive force directly, and to attempt to relate it to the α-effect. This procedure, however, is difficult to implement in theory and bound to be supremely inaccurate in practice; the fields are growing exponentially, are spatially varying, and can only be measured in the regime of interest for a limited amount of time ($t_1 < t < t_2$). A more sensible approach is to construct instead a family of experiments in which both the mean and fluctuations are stationary (in time), but which can be related to the experiment above. In this way the mean electromotive force can be measured to any desired accuracy by taking long enough samples. To motivate this construction we note that contributions to the mean electromotive force in the previous experiment are dominated by interactions between fluctuating quantities of vertical extent approximately $1/8$ the size of the box; over this scale the mean field ($K = 1$) is approximately uniform. Consequently, for this further series of experiments, we prescribe the mean field to be uniform and consider a computational domain of vertical extent $1/8$ that of the tall box. Details of the runs are given in table 2. Initially we assume that the imposed uniform magnetic field, of strength B_0, is in the vertical direction.

In this section, it is convenient to adopt the convention of measuring the (vertical) wavenumber in units of k_{max}, and hence we define $\hat{k} = k_z/k_{max}$. As in § 3, it is instructive to consider the roles of the nonlinear interactions so as to verify that the two cases are indeed analogous. Here the dominant magnetic fluctuations have $\hat{k} = 1$; their

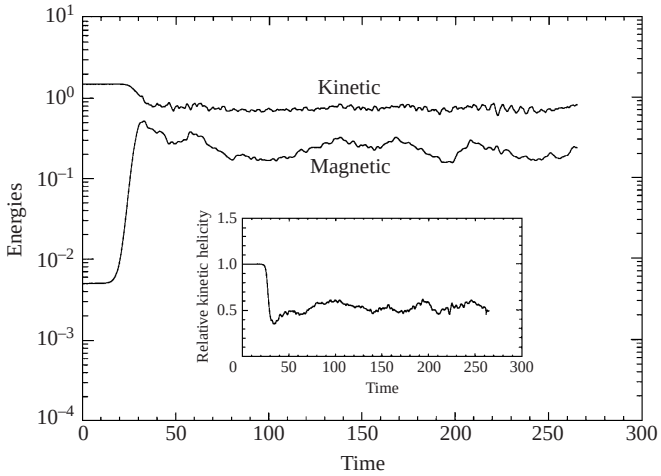

FIGURE 4. Time evolution of the magnetic and kinetic energies as functions of time for a case with $Rm = 200$, and $B_0^2 = 0.01$. The contributions to the magnetic energy arising from the dynamo instability exceed the energy of the uniform component at $t \approx 20$. At the same time the velocity begins to show substantial deviations from $\boldsymbol{U}_0$, and the kinetic helicity decreases. Shown in the inset is the time history of the *relative* kinetic helicity, $\langle \boldsymbol{U} \cdot \boldsymbol{\nabla} \times \boldsymbol{U} \rangle / \sqrt{\langle \boldsymbol{U}^2 \rangle \langle (\boldsymbol{\nabla} \times \boldsymbol{U})^2 \rangle}$.

	$B_0^2 = 10^{-4}$		$B_0^2 = 10^{-3}$		$B_0^2 = 10^{-2}$		$B_0^2 = 10^{-1}$		$B_0^2 = 1$	
Rm	U_{rms}	B_{rms}	U_{rms}	B_{rms}	U_{rms}	B_{rms}	U_{rms}	B_{rms}	U_{rms}	B_{rms}
25					1.39	0.91	1.26 (1.28)	0.61 (0.76)	1.37	1.19
50					1.32	0.79	1.23 (1.33)	0.59 (0.88)	1.38	1.24
100	1.40	1.08	1.33	0.93	1.29	0.72	1.23 (1.36)	0.51 (0.97)	1.38	1.30
200	1.33	0.87	1.28	0.80	1.27	0.68	1.19 (1.38)	0.63 (1.04)	1.36	1.36
300					1.27	0.68	1.24	0.64		

TABLE 2. The root-mean-square velocity U_{rms} and the root-mean-square magnetic field B_{rms} for various values of the vertical field B_0 and the magnetic Reynolds number Rm in the short box runs, with $Re = 100$, dimensions $2\pi \times 2\pi \times 2\pi/k_{max}$ and resolution 64^3. For runs with a horizontal field with $B_0^2 = 0.1$ the results are shown in parentheses.

interaction with the uniform ($\hat{k} = 0$) component of the magnetic field drives, via the Lorentz force, velocity fluctuations with $\hat{k} = 1$. It is then the interaction of the ($\hat{k} = 1$) magnetic and velocity fluctuations that contributes to the mean ($\hat{k} = 0$) electromotive force. We should note that, as in the previous case, the amplitude of the magnetic fluctuations is independent of the mean field, provided the latter is sufficiently weak, whereas the amplitude of the velocity fluctuations depends crucially on it. The main difference between the two cases is that here the mean electromotive force is generated by interactions between fluctuations with identical ($\hat{k} = 1$) wavenumbers, whereas in the evolution discussed in § 3.2 the contributions arise from interactions between neighbouring ($K = 8$ with $K = 7, 9$) wavenumbers.

The time history for a typical case ($Rm = 200$, $B_0^2 = 0.01$) is shown in figure 4. For early times the velocity is close to $\boldsymbol{U}_0$, and since there is no stretching of a uniform vertical field by a z-independent flow, the magnetic energy remains close to $B_0^2/2$. The amplitude of the fastest growing eigenmode ($\hat{k} = 1$) increases exponentially, its

contributions to the magnetic energy exceeding those of the imposed mean field at $t \approx 20$. At $t \approx 30$ the magnetic energy approaches the equipartition value and the dynamo growth saturates; after a period of nonlinear readjustment the system settles down to a stationary state. The relative kinetic helicity (inset in figure 4) initially has a value close to unity, corresponding to a maximally helical flow, decreasing to a value close to 0.5 in the nonlinear regime. In the stationary state, we define the volume-averaged electromotive force

$$\mathscr{E}(t) = \langle \boldsymbol{U} \times \boldsymbol{B} \rangle. \tag{4.1}$$

The quantity $\mathscr{E}$ is strongly fluctuating in time, and it would therefore be erroneous to use its value at any instant for the determination of α. Instead, we introduce its time average

$$\bar{\mathscr{E}}(T) = \frac{1}{T} \int_t^{t+T} \mathscr{E}(s) \mathrm{d}s. \tag{4.2}$$

This quantity should converge, for large T, to a value that is independent of t, and that can be meaningfully related to the α-effect since the mean field is time independent. An imposed vertical magnetic field allows the determination of three components of the α-tensor, thus we have

$$\alpha_{i3} = \bar{\mathscr{E}}_i / B_0. \tag{4.3}$$

Figure 5 shows the time histories of the z-, x- and y-components of $\mathscr{E}(t)$ and their time averages. We note that, as envisaged, the time averages are well behaved; the z-component eventually converges to a negative value (of opposite sign to the kinetic helicity), while the x- and y-components converge to zero, as indeed they must from symmetry considerations. By contrast, the quantity $\mathscr{E}(t)$ is strongly fluctuating, and it is clear that instantaneous readings, or short-term averages, could give rise to misleading results.

The results are summarized in figure 6, which shows the dependence of the non-zero component of α on the mean field energy. Each point on the graph corresponds to a long-time average of the type shown in figure 5. The results show a marked decrease in the efficiency of the α-effect once a critical, Rm-dependent value of the mean field strength is exceeded. In order to relate these results to those of § 3.2 we make a loose correspondence between time increasing from t_1 to t_2 in figure 3, and B_0^2 increasing in figure 6. At each instant, the effective value of α in the tall box experiment can be related to the value computed in the short box experiments for the corresponding value of B_0. It is now clear why the energy in the large-scale ($K = 1$) field saturates at a value much smaller than the equipartition value: the α-effect decreases by one order of magnitude over the range of interest ($10^{-4} \lesssim B_0^2 \lesssim 2 \times 10^{-2}$). An interesting feature of the data in figure 6 is that they make apparent the nonlinear character of the α-effect described in this study. In a truly kinematic situation the asymptotic value of the *turbulent* α-effect should be independent of Rm in the limit of vanishing B_0. In our case, however, the asymptotic values of α for the two cases differ by approximately a factor of three. We believe that this residual dependence on Rm, present even when the mean field is weak, is due to the fact that the part of the flow responsible for the α-effect is itself driven by the Lorentz force associated with the mean field. We can further verify that the critical value of the mean field strength above which suppression occurs depends on Rm by considering further cases for which Rm is varied for a fixed B_0 (figure 7). It should be noted that the lower two curves in figure 7 have no direct correspondence to the tall box experiment since the

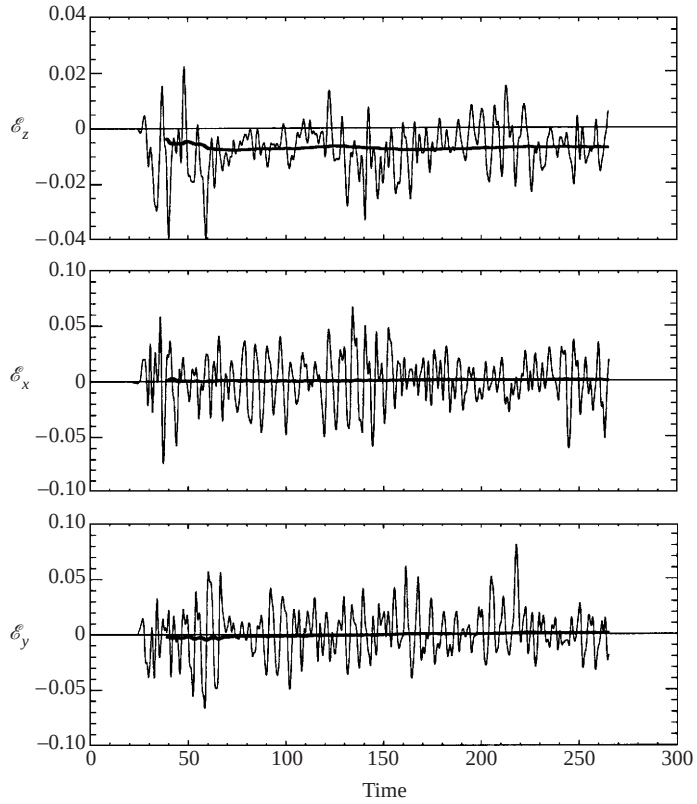

FIGURE 5. Time evolution of the z-, x- and y-components of the mean electromotive force $\mathscr{E}$ for a case with $Rm = 200$, and a uniform component of the magnetic field along the z-direction of strength given by $B_0^2 = 0.01$. The thick lines show the corresponding time averages. Notice that the z-component converges to a well defined *negative* value, i.e. of opposite sign to the average kinetic helicity, while the x- and y-components converge to zero.

value of the large-scale ($K = 1$) field never became strong enough to explore this region of parameter space.

Similar measurements can be made for the case when the imposed uniform field is horizontal, in the y-direction, say. This allows the determination of different components of the α-tensor. For instance, the existence of a mean electromotive force along the y-direction allows determination of α_{22}. However, since α is nonlinearly driven, this quantity is not the same as the corresponding component of the α-tensor for the case when the mean field is vertical. This property can be illustrated by comparing the value of α_{32} in the two cases. For the case of a vertical imposed field, α_{23} can be explicitly computed to be zero (see figure 5). For the system under consideration, which is statistically homogeneous along each direction separately, it is reasonable to assume that the α-tensor is symmetric (Moffatt 1978), and thus we can infer that α_{32} is also zero. This should be contrasted with the value of α_{32} calculated for an imposed field in the y-direction, which is manifestly non-zero, as shown in figure 8. These considerations notwithstanding, as shown in figure 9, the behaviour of the α-effect, though not identical, remains qualitatively the same, with strong suppression occurring once the mean field exceeds a (small) Rm-dependent value.

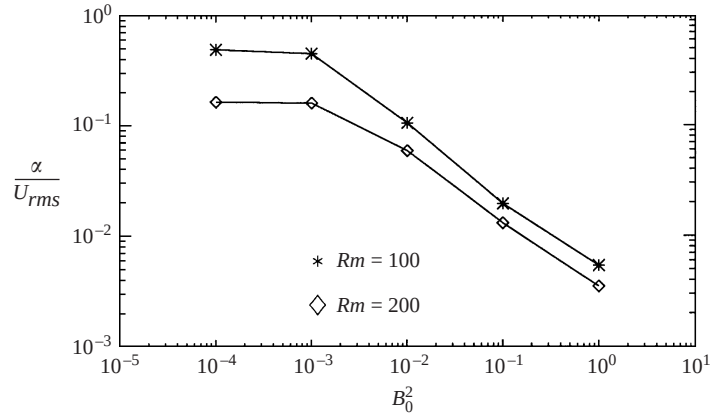

FIGURE 6. Non-zero component of the α-effect computed from the time-averaged mean electromotive force as a function of B_0^2 for cases in which the uniform component of the magnetic field is in the z-direction. Each marked point corresponds to a distinct numerical experiment. The value of the α-effect has been normalized with respect to the r.m.s. velocity for each case.

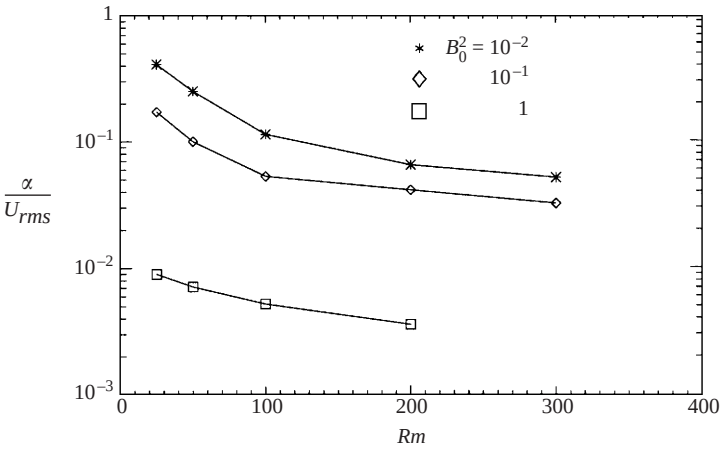

FIGURE 7. Non-zero component of the α-effect computed from the time-averaged mean electromotive force as a function of Rm for cases in which the uniform component of the magnetic field is in the z-direction. Each marked point corresponds to a distinct numerical experiment. The value of the α-effect has been normalized with respect to the r.m.s. velocity for each case.

5. Discussion

The results of the previous sections present us with a number of issues that deserve discussion. One of the many significant conclusions to be drawn from the tall box calculations of § 3 is that nonlinear dynamo states depend crucially on initial conditions. This is true even when the initial conditions describe a state of weak magnetization. In general terms, one of the determining factors appears to be the distribution of magnetic energy among the different scales at the time when the strongest fluctuations reach equipartition. For example, in the first experiment (§ 3.1) there was little further growth of the small-scale components once the large-scale component had saturated. By contrast, in the second experiment the growth of the large-scale component was accelerated, albeit only for a short time, by the presence of small-scale fluctuations at the equipartition level. We should point out that our chief interest in this work has been in the magnetic field evolution on short

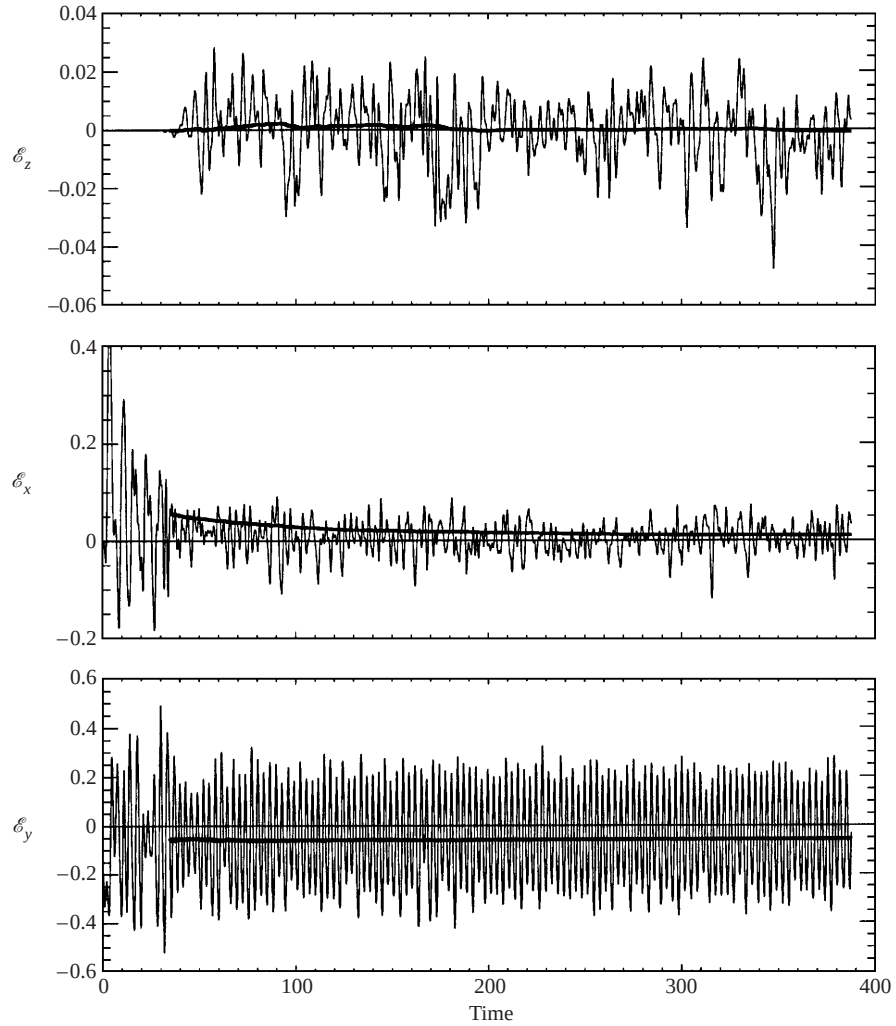

FIGURE 8. Time evolution of the z-, x- and y-components of the mean electromotive force $\mathscr{E}$ for a case with $Rm = 100$, and a uniform component of the magnetic field along the y-direction of strength given by $B_0^2 = 0.01$. The thick lines show the corresponding time averages. Notice that the y- and x-components converge to well-defined non-zero values, while the z-component converges to zero.

dynamical timescales. There is, though, also evidence for readjustments on a much longer timescale. For instance, in the second experiment of § 3 the total magnetic energy continues to increase after what we have called the nonlinear saturation phase. However, the growth is extremely slow, and, although one cannot be absolutely certain from simulations conducted at a moderate value of Rm, appears to be occurring on an Ohmic diffusion timescale. This idea is reinforced by the dynamo simulations of Brandenburg (2001) who considers a range of Rm (again, of necessity, restricted to small to moderate values) and who finds a long-term adjustment on a timescale that increases with Rm. This slow growth in magnetic energy is also accompanied by changes in field geometry; for instance, modes with different wavenumbers may occasionally swap amplitude (see figure 3). It is by no means clear whether a unique

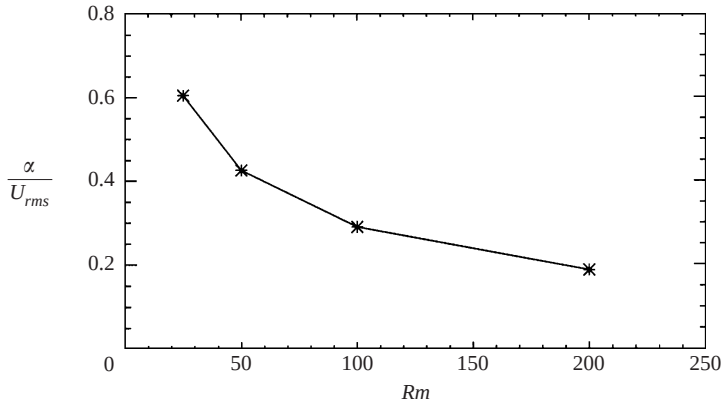

FIGURE 9. Largest non-zero component of the α-effect (α_{22}) computed from the time-averaged mean electromotive force as a function of *Rm* for cases in which the uniform component of the magnetic field is in the y-direction and $B_0^2 = 0.1$. Each marked point corresponds to a distinct numerical experiment. The value of the α-effect has been normalized with respect to the r.m.s. velocity for each case.

final state is achieved. The present evidence, such as it is, suggests that this is unlikely. We have deliberately chosen not to study this aspect of the dynamo problem for two reasons. In most astrophysical situations the Ohmic timescale is very long, and dynamo theory concentrates on the problem of field generation on dynamical timescales. Furthermore, even though the problem is of some interest, it is impractical to pursue its study by high-resolution numerical simulations.

One of the interesting features of the early phases of the simulations concerns the nature of the kinematic approximation. In nonlinear dynamo simulations starting from initial conditions of weak magnetization, it is conventional to distinguish an initial kinematic regime from a subsequent dynamical regime, the former being identified as the time period during which the Lorentz force is dynamically insignificant. Typically, this phase of the evolution is described by the kinematic approximation, which consists of solving the induction equation alone, for a prescribed velocity field. There are circumstances, however, in which this procedure is inappropriate, corresponding to cases in which the Lorentz force, though dynamically insignificant, has important symmetry-breaking effects. For these cases, paradoxically, the kinematic regime cannot adequately be described by the kinematic approximation. For example, in the tall box experiments, it is the action of the Lorentz force that is responsible for the generation and rapid amplification of all the modes with wavenumbers K not equal to 1 or 8. If we had instead described the 'kinematic' evolution in terms of the induction equation alone, the distribution of energy between the different wavenumbers at the time when the Lorentz force became dynamically significant would have been very different, with radical consequences for the subsequent evolution.

The evolution of the large-scale magnetic field described in § 3.2 is consistent with the existence of an α-effect that is driven nonlinearly, and whose efficiency decreases dramatically once the mean field energy exceeds a critical value. This interpretation is further supported by the small box experiments showing that an α-effect with precisely these properties can be measured to any degree of accuracy, provided a correspondence is made between volume averaging in the tall boxes, and time averaging in the small ones. Furthermore, there is an agreement between the tall box and short box experiments regarding the mean field intensity above which the

α-effect becomes inoperative. Significantly, this value agrees with the notion that the α-effect is strongly nonlinearly suppressed (Vainshtein & Cattaneo 1992; Kulsrud & Anderson 1992; Gruzinov & Diamond 1995; Cattaneo & Hughes 1996). Because so many models of astrophysical dynamos rely on the concept of an α-effect, it is worthwhile to speculate about the general applicability of the above result.

The idea that the turbulent α-effect could be strongly suppressed (i.e. that a weak, *Rm*-dependent, field could have an $O(1)$ influence on α) was initially suggested by analogy with the strong suppression of the turbulent diffusivity in two-dimensional MHD (Vainshtein & Cattaneo 1992; Cattaneo & Vainshtein 1992). This result was further supported by independent studies based on quasi-linear closures (Gruzinov & Diamond 1995), and by numerical simulations similar to the short box experiments described above (Cattaneo & Hughes 1996). These conclusions have, however, been challenged by the work of Blackman, Field and coworkers, who have raised two types of objections. Field, Blackman & Chou (1999) claimed that the strong suppression result was incorrect, despite its excellent agreement with numerical experiments. However it should be noted that the results of Field *et al.* (1999) are based on an assumption that the Strouhal number, S, defined as the ratio of the eddy correlation time to the eddy turnover time, is small. This assumption is certainly incorrect for hydrodynamic turbulence where it is known experimentally that S is $O(1)$. Little is known experimentally about the magnitude of S in the *hydromagnetic* case for large *Rm*. However it is not likely to be smaller than in the *hydrodynamic* case, and, indeed, some numerical evidence suggests that it may actually be large (Cattaneo 1994); thus the approach of Field *et al.* (1999) may well be fatally flawed. In a later work, Blackman & Field (2000) changed the nature of their objection, arguing instead that the strong suppression result was, after all, correct – a stark contradiction to their earlier claim – but was inapplicable to astrophysical situations. Instead, they claim that the dependence of α on *Rm* and B_0 observed by Cattaneo & Hughes (1996) 'is not a dynamic suppression' and that the dominant nonlinear influence on α results instead from the role of magnetic helicity flux through the boundaries of the dynamo region. The first of these assertions is completely false – the suppression measured by Cattaneo & Hughes (1996) arises entirely as a result of the Lorentz force and hence is a totally dynamic phenomenon. As for the second point, it is certainly plausible that the helicity flux plays some role in determining α. However, just how important a role depends crucially on the nature of the term describing this flux. At the moment, there are no estimates of its magnitude relative to that of the term describing the suppression. We believe that these should emerge either from a rigorous theory of MHD turbulence – not likely to be forthcoming – or from careful numerical experiments. Until such results become available, the authors would like to keep a healthy state of neutrality on the matter.

We conclude this paper by returning to the initial motivation for this work, namely the generation of large-scale magnetic fields by small-scale turbulence. The traditional viewpoint, going back to the work of Pouquet, Frish & Léorat (1976), is that the saturation process proceeds from small to large scales as each scale reaches equipartition. In this scenario the inverse cascade responsible for the transfer of magnetic energy to larger scales remains efficient, and large-scale fields of equipartition amplitude can readily be generated. By contrast, within the present framework it would appear that it is difficult to generate a large-scale magnetic field of substantial amplitude unless one is already present at the onset of the dynamical regime. In that case (§ 3.1) the nature of the saturation is such as to inhibit the further amplification of magnetic fields on all smaller scales. In view of this fact, we would like to propose

the following nonlinear dynamo conjecture: when dynamo saturation occurs on a given scale it inhibits the growth of magnetic fields on smaller, but not necessarily on larger scales. For instance, for helical turbulence, a large-scale magnetic field could be amplified even after the nonlinear saturation of the small-scale field. However, as seen in the present numerical experiments, this mechanism itself becomes ineffective at small amplitudes of the large-scale field.

We would like to thank Drs N. H. Brummell and S. M. Tobias, and Professors M. R. E. Proctor, R. Rosner, and N. O. Weiss for many useful discussions. F. C. was supported in part by the NASA SR&T program, the DOE Flash initiative at the University of Chicago, and PPARC, D. W. H. was supported in part by PPARC, and J. C. T. was supported by the NASA SR&T and TRACE programs at the University of Chicago.

REFERENCES

Blackman, E. G. & Field, G. B. 2000 Constraints on the magnitude of alpha in dynamo theory. *Astrophys. J.* **534**, 984–988.

Brandenburg, A. 2001 The inverse cascade and nonlinear alpha-effect in simulations of isotropic helical hydromagnetic turbulence. *Astrophys. J.* **550**, 824–840.

Cattaneo, F. 1994 On the effects of a weak magnetic field on turbulent transport. *Astrophys. J.* **434**, 200–205.

Cattaneo, F. & Hughes, D. W. 1996 Nonlinear saturation of the turbulent α effect. *Phys. Rev.* E **54**, R4532–R4535.

Cattaneo, F., Kim, E., Proctor, M. R. E. & Tao, L. 1995 Fluctuations in quasi-2-dimensional fast dynamos. *Phys. Rev. Lett.* **75**, 1522–1525.

Cattaneo, F. & Vainshtein, S. I. 1992 Suppression of turbulent transport by a weak magnetic field. *Astrophys. J.* **376**, L21–L24.

Field, G. B., Blackman, E. G. & Chou, H. S. 1999 Nonlinear alpha-effect in dynamo theory. *Astrophys. J.* **513**, 638–651.

Galloway, D. J. & Proctor, M. R. E. 1992 Numerical calculations of fast dynamos in smooth velocity fields with realistic diffusion. *Nature* **356**, 691–693.

Gruzinov, A. V. & Diamond, P. H. 1995 Self-consistent mean-field electrodynamics of turbulent dynamos. *Phys. Plasmas* **2**, 1941–1946.

Hughes, D. W., Cattaneo, F. & Kim, E. 1996 Kinetic helicity, magnetic helicity and fast dynamo action. *Phys. Lett.* A **223**, 167–172.

Hughes, D. W., Cattaneo, F. & Kim, E. 1998 Nonlinear multi-cellular fast dynamos. *Stud. Geophys. Geod.* **42**, 328–334.

Krause, F. & Rädler, K.-H. 1980 *Mean-Field Magnetohydrodynamics and Dynamo Theory*. Pergamon.

Kulsrud, R. M. & Anderson, S. W. 1992 The spectrum of random magnetic fields in the mean field dynamo theory of the galactic magnetic field. *Astrophys. J.* **396**, 606–630.

Moffatt, H. K. 1978 *Magnetic Field Generation in Electrically Conducting Fluids*. Cambridge University Press.

Otani, N. F. 1993 A fast kinematic dynamo in 2-dimensional time-dependent flows. *J. Fluid Mech.* **253**, 327–340.

Parker, E. N. 1979 *Cosmical Magnetic Fields*. Clarendon Press.

Podvigina, O. & Pouquet, A. 1994 On the nonlinear stability of the 1/1/1/ *ABC* flow. *Physica* D **75**, 471–508.

Ponty, Y., Pouquet, A. & Sulem, P. L. 1995 Dynamos in weakly chaotic 2-dimensional flows. *Geophys. Astrophys. Fluid Dyn.* **79**, 239–257.

Pouquet, A., Frisch, U. & Léorat, J. 1976 Strong MHD helical turbulence and the nonlinear dynamo effect. *J. Fluid Mech.* **77**, 321–354.

Soward, A. M. 1987 Fast dynamo action in a steady flow. *J. Fluid Mech.* **180**, 267–295.

Vainshtein, S. I. & Cattaneo, F. 1992 Nonlinear restrictions on dynamo action. *Astrophys. J.* **393**, 165–171.